

| | |
|-------------|---|
| Title | Effects of side groups on the entanglement network of cellulosic polysaccharides |
| Author(s) | Horinaka, Jun-ichi; Urabayashi, Yuhei; Takigawa, Toshikazu |
| Citation | Cellulose (2015), 22(4): 2305-2310 |
| Issue Date | 2015-05-27 |
| URL | http://hdl.handle.net/2433/201993 |
| Right | The final publication is available at Springer via http://dx.doi.org/10.1007/s10570-015-0670-7 .; The full-text file will be made open to the public on 27 May 2016 in accordance with publisher's 'Terms and Conditions for Self-Archiving'. |
| Type | Journal Article |
| Textversion | author |

1 **Effects of side groups on entanglement network of cellulosic polysaccharides**

2

3 Jun-ichi Horinaka*, Yuhei Urabayashi, and Toshikazu Takigawa

4

5 Department of Material Chemistry, Graduate School of Engineering, Kyoto University,

6 Nishikyo, Kyoto 615-8510, Japan

7

8

9 * Corresponding author.

10 E-mail: horinaka.junichi.5c@kyoto-u.ac.jp

11 Tel: +81-75-383-2454

12 Fax: +81-75-383-2458

13

14

15

16

17

18

19 **Abstract**

20 The transient entanglement network of cellulosic polysaccharides in concentrated solutions
21 were characterized by the molecular weight between entanglements (M_e) using dynamic
22 viscoelasticity measurements. From the concentration dependence of M_e , M_e for the cellulosic
23 polysaccharides in the molten state ($M_{e,melt}$) was estimated as the material constants reflecting
24 the chain characteristics. The values of $M_{e,melt}$ were compared among three cellulosic
25 polysaccharides: cellulose, methylcellulose, and hydroxypropyl cellulose. Methylcellulose and
26 hydroxypropyl cellulose were employed as cellulose derivatives having small and large side
27 groups, respectively. It appeared that hydroxypropyl cellulose had significantly larger $M_{e,melt}$
28 compared with cellulose and methyl cellulose. However, the numbers of repeating glucose-ring
29 units between entanglements were very close to each other among the three polysaccharides.

30

31

32

33

34 **Keywords** entanglement network· cellulosic polysaccharide· side group· concentrated
35 solution· molecular weight between entanglements

36

37

38

39 **Introduction**

40 Cellulose is the most familiar polysaccharide as the result of long years of use in human history.

41 In addition to cellulose in the natural form, many derivatives are known to be synthesized from

42 cellulose by modifying the hydroxyl groups. The main aim of introducing the substituents is to

43 change the physical properties of cellulose; for example, methylcellulose is water-soluble in

44 contrast to natural cellulose, because the methyl groups reduce the strength of hydrogen

45 bonding between cellulose chains. Currently, cellulosic polysaccharides, meaning cellulose as

46 well as its derivatives, are vital materials in several industries due to the various properties.

47 Cellulosic polysaccharides are also of interest in the field of chain characterization of

48 polymers. The chain dimensions of cellulosic polysaccharides in various dilute solutions have

49 been examined previously and the effects of side groups (substituents) on the unperturbed chain

50 parameters as well as on the hydrodynamic properties have been discussed based on the

51 accumulated data (Brown et al. 1963; Brown et al. 1964; Flory 1966; Kamide et al. 1978;

52 Kamide et al. 1987). Thus chain characterization of cellulosic polysaccharides using dilute

53 solutions has been successfully carried out. Studies on concentrated systems of cellulosic

54 polysaccharides are also making good progress (Chen et al. 2009; Gericke et al. 2009; Haward

55 et al. 2012; Kosan et al. 2008; Syang-Peng et al. 2009). A specific matter to concentrated

56 polymer systems such as polymer melts and concentrated solutions is the entanglement coupling

57 between polymer chains emerging from topological constraints of the interpenetrating polymer
58 chains. It is recognized that entanglement coupling dominates the rheological behavior of
59 concentrated polymer systems at long times (Doi et al. 1986; Ferry 1980). The entanglement
60 coupling can be characterized by the molecular weight between entanglements (M_e), which
61 corresponds to an average mesh size of the transient entanglement network. The value of M_e for
62 a polymer melt ($M_{e,melt}$) especially is a material constant; namely, $M_{e,melt}$ is a type of chain
63 characteristics obtained only by examining the rheological behavior of concentrated polymer
64 systems. Until now, however, $M_{e,melt}$ for the better part of cellulosic polysaccharides have been
65 unknown and effects of side groups on entanglement coupling for cellulosic polysaccharides has
66 not even been considered.

67 In this paper, $M_{e,melt}$ for three cellulosic polysaccharides, cellulose (C), methylcellulose (MC),
68 and hydroxypropyl cellulose (HPC), have been estimated from the rheological data for their
69 concentrated solutions. It should be noted that MC has small substituents of methyl groups,
70 while HPC has larger ones of hydroxypropyl groups, which is characterized by the molecular
71 weight of a repeating unit (M_{unit}) below. Use of an ionic liquid as a solvent has made it possible
72 to prepare solutions of these cellulosic polysaccharides at high concentrations where there is
73 entanglement coupling. The values of $M_{e,melt}$ as well as the number of repeating glucose-ring
74 units between entanglements (N_{unit}) have been compared among the three polysaccharides.

75

76 **Experimental**

77 **Materials**

78 The cellulosic polysaccharides, C (Aldrich, USA), MC (Aldrich, USA), and HPC (Wako, Japan),
79 were used without further purification. According to the manufacturers, the degree of
80 substitution per repeating unit were 1.7 and 3.8 for MC and HPC, respectively; therefore, M_{unit}
81 for C, MC, and HPC were estimated to be 162, 186, and 383, respectively. The viscosities for
82 2 % aqueous solutions of MC and HPC at 20 °C were reported by the manufacturers to be 4000
83 cP and 1000-4000 cP, respectively, whereas that for C was unavailable. An ionic liquid
84 1-butyl-3-methylimidazolium acetate (BmimAc; BASF, Germany) was used as received. As far
85 as we tested, BmimAc was the only common solvent to prepare concentrated solutions of the
86 three polysaccharides. Each polysaccharide sample was added into liquid BmimAc in a dry
87 glass vessel, and then the mixture was stirred on a hot plate at about 80 °C for more than 6 h
88 until complete dissolution. The concentration of the polysaccharides (c) ranged from 1.1×10^2
89 to $2.1 \times 10^2 \text{ kgm}^{-3}$ (ca. 10 to 20 wt %) for C, from 4.2×10^1 to $7.5 \times 10^1 \text{ kgm}^{-3}$ (ca. 4 to 7 wt %)
90 for MC, from 5.2×10^1 to $2.6 \times 10^2 \text{ kgm}^{-3}$ (ca. 5 to 25 wt %) for HPC; the lowest c was slightly
91 above the critical concentration for entanglement coupling, while the highest c was determined
92 by the solubility. In the calculation of c , the densities of melts of the polysaccharides were

93 commonly assumed to be $1.0 \times 10^3 \text{ kgm}^{-3}$ and that of BmimAc was quoted to be 1.055×10^3
94 kgm^{-3} (Horinaka et al. 2013).

95

96 Rheological measurements

97 The angular frequency (ω) dependence of the storage modulus (G') and the loss modulus (G'')

98 for the polysaccharide solutions was measured with an ARES rheometer (now TA Instruments,

99 USA) under a nitrogen atmosphere. The geometry for the measured sample was a cone-plate

100 with a diameter of 25 mm and a cone angle of 0.1 rad. The value of ω ranged from 0.1 to 100 s^{-1}

101 and the amplitude of the oscillatory strain (γ) was fixed at 0.1 so that the measurement could be

102 performed in the linear viscoelasticity region. The above measurement was carried out at several

103 temperatures (T) from 0 to $80 \text{ }^\circ\text{C}$.

104

105 **Results and Discussion**

106 Figure 1 shows the ω dependence of G' and G'' for the C solutions; the curves are shifted

107 upwards by A to avoid overlapping for different c . Each of the curves is the so-called master

108 curve at the reference temperature (T_r) of $80 \text{ }^\circ\text{C}$ obtained by means of a horizontal shift by a

109 factor of a_T for each T according to the frequency-temperature superposition principle. It

110 appears that the time-temperature superposition principle holds well for the C solutions. At low

111 ωa_T , flow of the system can be seen for each c , although the terminal relation of $G'' \propto \omega$ is
112 observed only for the solution of $c = 1.1 \times 10^2 \text{ kgm}^{-3}$. In the middle ωa_T region, there is a
113 plateau region in each G' curve where $G' > G''$, which becomes wider as c increases; this is the
114 so-called rubbery plateau, indicating the existence of entanglements coupling in the C solutions.
115 The reason that the plateau of G' is slightly tilted is probably the polydispersity of the sample
116 employed, although actual data on the polydispersity are not available. In Figures 2, $\log a_T$ is
117 plotted against $1/T$. All data points can be fitted by a single line regardless of c , as drawn in the
118 figure, indicating that the T -dependence curve of a_T can be represented by an Arrhenius-type
119 equation. This trend implies that the solutions are homogeneous.

120 Figure 3 shows the master curves of the ω dependence of G' and G'' at $T_r = 80 \text{ }^\circ\text{C}$ for the MC
121 solutions obtained in the similar way to Figure 1. Although the rubbery plateau region in each
122 G' curve is not obvious compared with that in Figure 1 partly due to the low c , the rubbery
123 plateau as well as the flow region is seen for each c in the G' and G'' curves, which is typical of
124 polymer solutions with entanglement coupling. The T -dependence curve of a_T for the MC
125 solutions is shown in Figure 4. The values of a_T at a given T are almost identical regardless of c ,
126 and all data points in the figure appear to fall on a single line.

127 The master curves of the ω dependence of G' and G'' at $T_r = 80 \text{ }^\circ\text{C}$ for the HPC solutions are
128 given in Figure 5. The rubbery plateau region becomes wider as c increases, so that the flow

129 region goes out of sight for the solution of $c = 2.1 \times 10^2 \text{ kgm}^{-3}$. The Arrhenius-type plot of a_T
 130 for the HPC solutions is shown in Figure 6. As is the case of C and MC, the data points fall on a
 131 single line; namely, a_T for these solutions show almost the same T -dependence being
 132 independent of c . This result supports that the HPC solutions are homogeneous within the c
 133 range examined.

134 As demonstrated above, the rubbery plateau appears for all the solutions examined. From the
 135 analogy with the rubber elasticity, M_e (in gmol^{-1}) for a polymer in solution at the concentration
 136 of c can be given by

$$137 \quad M_e = \frac{10^3 cRT}{G_N^0} \quad (1)$$

138 Here, G_N^0 is the plateau modulus, which corresponds to the height of the plateau, and R is the
 139 gas constant (Doi et al. 1986; Ferry 1980). It should be noted that G_N^0 is independent of the
 140 molecular weight of the polymer itself as long as the molecular weight is sufficiently greater
 141 than $2M_e$ and the plateau appears (Ferry 1980; Onogi 1970). As seen in the above figures, the
 142 actual plateaus obtained in this study were tilted to some extent, and therefore we defined G_N^0
 143 as the G' value at ωa_T where the loss tangent ($\tan \delta = G''/G'$) attained the minimum in the
 144 rubbery plateau region (Horinaka et al. 2011; Horinaka et al. 2013). For example, G_N^0 for the
 145 HPC solution at $c = 2.1 \times 10^2 \text{ kgm}^{-3}$ is determined to be $1.9 \times 10^4 \text{ Pa}$ in Figure 5, which gives
 146 M_e of 3.2×10^4 from eq. 1 with $T = T_r$. The values of M_e for the C, MC, and HPC solutions

147 obtained in this manner are double-logarithmically plotted against c in Figure 7. For each
148 polysaccharide, a straight line with a slope of -1 is drawn with the best fit method, because it
149 has been reported that a relation of $M_e \propto c^{-1}$ holds for many concentrated solutions of polymers
150 (Doi et al. 1986; Masuda et al. 1972). It is seen that data points in the figure are fitted well by
151 the line, indicating that the $M_e \propto c^{-1}$ relation also holds for the C, MC, and HPC solutions
152 examined in this study. Hence, $M_{e,melt}$ for the cellulosic polysaccharides can be estimated to be
153 M_e at $c = 1.0 \times 10^3 \text{ kgm}^{-3}$ of the fitted line in Figure 7 as we assume the density of the
154 polysaccharides to be $1.0 \times 10^3 \text{ kgm}^{-3}$. The obtained values of $M_{e,melt}$ are 2.9×10^3 , 2.5×10^3 ,
155 and 6.2×10^3 for C, MC, and HPC, respectively. Here, it is noted that $M_{e,melt}$ for C estimated in
156 the current study is consistent within the experimental error with that for C obtained in our
157 previous study where another ionic liquid 1-butyl-3-methylimidazolium chloride has been used
158 as the solvent (Horinaka et al. 2011; Horinaka et al. 2012). The value of $M_{e,melt}$ for MC obtained
159 in this study is slightly smaller than that for C. Considering the experimental error, this
160 difference might be negligible. On the other hand, $M_{e,melt}$ for HPC is significantly larger. These
161 results suggest that the effects of side groups on $M_{e,melt}$ are apparent but not monotonous against
162 M_{unit} . It has been reported earlier that there is an irregular tendency for the effect of M_{unit} on a
163 chain stiffness parameter of cellulosic polysaccharides in dilute solutions, although direct
164 comparison with our result is impossible (Brown et al. 1964). It should be noted that

165 aggregation behavior of the cellulosic polysaccharides does not account for the difference in
166 $M_{e,melt}$. It has been reported that side groups of cellulosic polysaccharides affects the solubility in
167 conventional solvents and extremely high substitution is necessary to obtain the molecularly
168 dissolved solutions (Burchard 2003). For the ionic liquid solutions of cellulosic polysaccharides,
169 it is recognized that dissolution on the molecular level is achieved by forming hydrogen bonds
170 between the anions of the solvent and the hydroxyl protons of the solute, and therefore even
171 cellulose can be molecularly dissolved in ionic liquids, as demonstrated by a light scattering
172 study (Chen et al. 2011; Swatloski, Spear, Holbrey, Rogers 2002). Our results in Figures 1, 3,
173 and 5 also indicate that there are no aggregates of the polysaccharides in all the solutions
174 examined in this study; if the aggregates exist in the solution, another plateau (or at least
175 shoulder), the so-called second plateau, should appear in the flow region before reaching the
176 terminal behavior. Maeda et al. have explained the dynamic viscoelasticity data for an ionic
177 liquid solution of cellulose over a wide range of frequency from the flow to the glassy zone
178 successfully without taking the aggregated state of cellulose into consideration (Maeda, Inoue,
179 Sato 2013). Now, we consider N_{unit} instead of $M_{e,melt}$. Since cellulosic polysaccharides have a
180 common backbone structure of repeating glucose-ring units, the contour length between
181 entanglement coupling points can be compared using N_{unit} . In other words, N_{unit} represents the
182 mesh size of the entanglement network in terms of length. The values of N_{unit} calculated from

183 $M_{e,melt}$ and M_{unit} are 18, 13, and 16 for C, MC, and HPC, respectively. The values of N_{unit} come
184 closer to each other compared with $M_{e,melt}$.

185

186 **Conclusions**

187 The effects of side groups on entanglement network of cellulosic polysaccharide were examined
188 in terms of the rheological properties $M_{e,melt}$ and N_{unit} . Dynamic viscoelasticity measurements for
189 the concentrated solutions of C, MC, and HPC in BmimAc provided $M_{e,melt}$ of 2.9×10^3 , $2.5 \times$
190 10^3 , and 6.2×10^3 , respectively, indicating that there was an dependence of $M_{e,melt}$ on M_{unit} ,
191 although the dependence appeared rather complicated. On the other hand, the effects of side
192 groups were very small regarding N_{unit} .

193

194 **References**

195 Brown W, Henry D, Ohman J (1963) Studies on cellulose derivatives part II. The influence of
196 solvent and temperature on the configuration and hydrodynamic behavior of hydroxyethyl
197 cellulose in dilute solution. Makromol Chem 64: 49-67

198 Brown W, Henry D (1964) Studies on cellulose derivatives part III. Unperturbed dimensions of
199 hydroxyethyl cellulose and other derivatives in aqueous solvents. Makromol Chem 75:
200 179-188

201 Burchard W (2003) Solubility and solution structure of cellulose derivatives. *Cellulose*
202 10:213-225.

203 Chen X, Zhang Y, Cheng L, Wang H (2009) Rheology of concentrated cellulose solutions in
204 1-butyl-3-methylimidazolium chloride. *J Polym Environ* 17: 273-279

205 Chen X, Zhang Y, Ke F, Zhou J, Wang H, Liang D (2011) Solubility of neutral and charged
206 polymers in ionic liquids studied by laser light scattering. *Polymer* 52: 481-488

207 Doi M, Edwards SF (1986) *The theory of polymer dynamics*. Clarendon Oxford

208 Ferry JD (1980) *Viscoelastic properties of polymers*. John Wiley and Sons New York

209 Flory PJ (1966) Treatment of the effect of excluded volume and deduction of unperturbed
210 dimensions of polymer chains. Configurational parameters for cellulose derivatives.
211 *Makromol Chem* 98: 128-135

212 Gericke M et al. (2009) Rheological properties of cellulose/ionic liquid solutions: from dilute to
213 concentrated states. *Biomacromolecules* 10: 1188-1194.

214 Haward SJ et al. (2012) Shear and Extensional Rheology of Cellulose/Ionic Liquid Solutions.
215 *Biomacromolecules* 13: 1688-1699

216 Horinaka J, Yasuda R, Takigawa T (2011) Entanglement properties of cellulose and amylose in
217 an ionic liquid. *J Polym Sci B Polym Phys* 49: 961-965

218 Horinaka J, Okuda A, Yasuda R, Takigawa T (2012) Molecular weight between entanglements

- 219 for linear D-glucans. *Colloid Polym Sci* 290: 1793-1797
- 220 Horinaka J, Urabayashi Y, Takigawa T, Ohmae M (2013) Entanglement network of chitin and
221 chitosan in ionic liquid solutions. *J Appl Polym Sci* 130: 2439-2443
- 222 Kamide K, Miyazaki Y (1978) The partially free draining effect and unperturbed chain
223 dimensions of cellulose, amylose, and their derivatives. *Polym J* 10: 409-431
- 224 Kamide K, Saito M (1987) Cellulose and cellulose derivatives: recent advances in physical
225 chemistry. *Adv Polym Sci* 83: 1-56
- 226 Kosan B, Michels C, Meister F (2008) Dissolution and forming of cellulose with ionic liquids.
227 *Cellulose* 15: 59-66
- 228 Meda A, Inoue T, Sato T (2013) Dynamic segment size of the cellulose chain in an ionic liquid.
229 *Macromolecules* 46: 7118-7124
- 230 Masuda T, Toda N, Aoto Y, Onogi S (1972) Viscoelastic properties of concentrated solutions of
231 poly(methyl methacrylate) in diethyl phthalate. *Polym J* 3: 315-321
- 232 Onogi S, Masuda T, Kitagawa K (1970) Rheological properties of anionic polystyrenes. I.
233 dynamic viscoelasticity of narrow-distribution polystyrenes. *Macromolecules* 3: 109-116
- 234 Swatloski RP, Spear SK, Holbrey JD, Rogers RD (2002) Dissolution of cellose with ionic
235 liquids. *J Am Chem Soc* 124: 4974-4975
- 236 Syang-Peng R et al. (2009) Sol/gel transition and liquid crystal transition of HPC in ionic liquid.

237 Cellulose 16: 9-17

238

239

240 Figure Captions

241 **Fig. 1** Master curves of ω dependence of G' and G'' for the C solutions at $T_r = 80$ °C. The
242 curves are shifted upwards by A .

243 **Fig. 2** Shift factor for the C solutions plotted against the reciprocal of T . All data points fall on
244 a single line.

245 **Fig. 3** Master curves of ω dependence of G' and G'' for the MC solutions at $T_r = 80$ °C. The
246 curves are shifted upwards by A .

247 **Fig. 4** Shift factor for the MC solutions plotted against the reciprocal of T . All data points fall
248 on a single line.

249 **Fig. 5** Master curves of ω dependence of G' and G'' for the HPC solutions at $T_r = 80$ °C. The
250 curves are shifted upwards by A .

251 **Fig. 6** Shift factor for the HPC solutions plotted against the reciprocal of T . All data points fall
252 on a single line.

253 **Fig. 7** Double-logarithmic plot of M_e vs. c for the cellulosic polysaccharides in solution. Each
254 line is the best fit one with a slope of -1 . $M_{e,melt}$ is defined as M_e at $c = 10^3$ kgm⁻³.

255

Figure 1

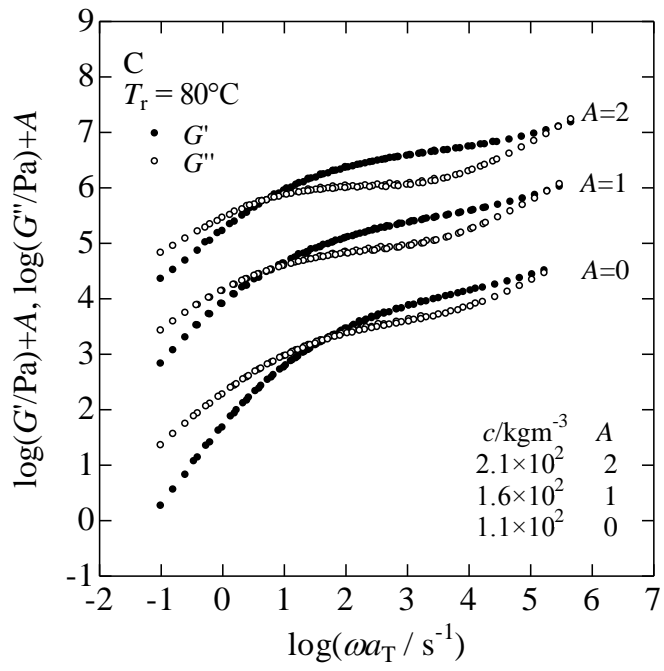


Figure 2

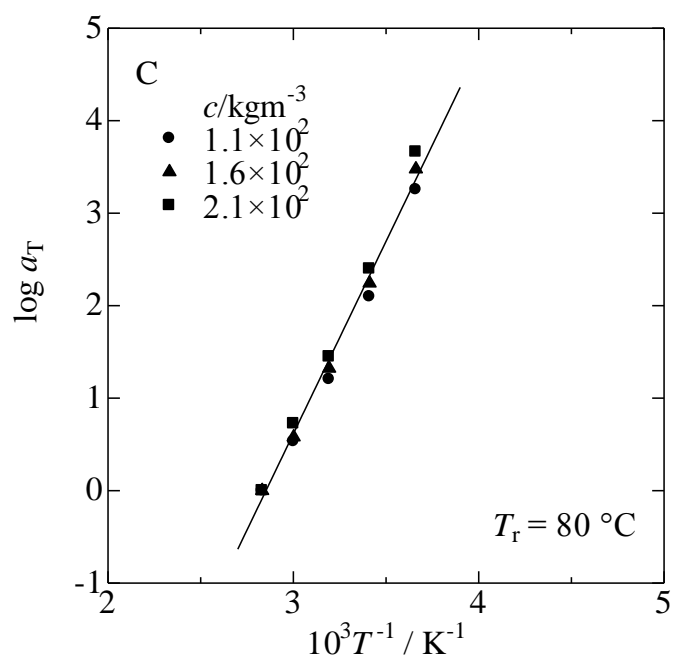


Figure 3

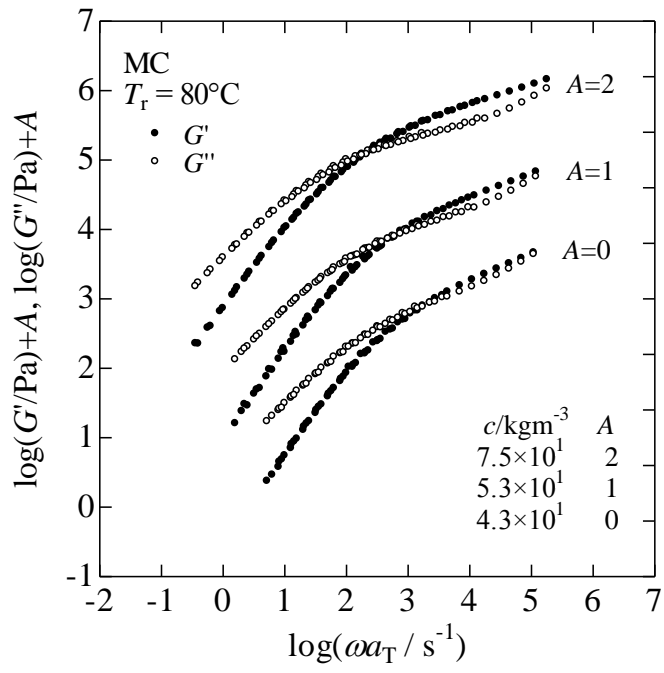


Figure 4

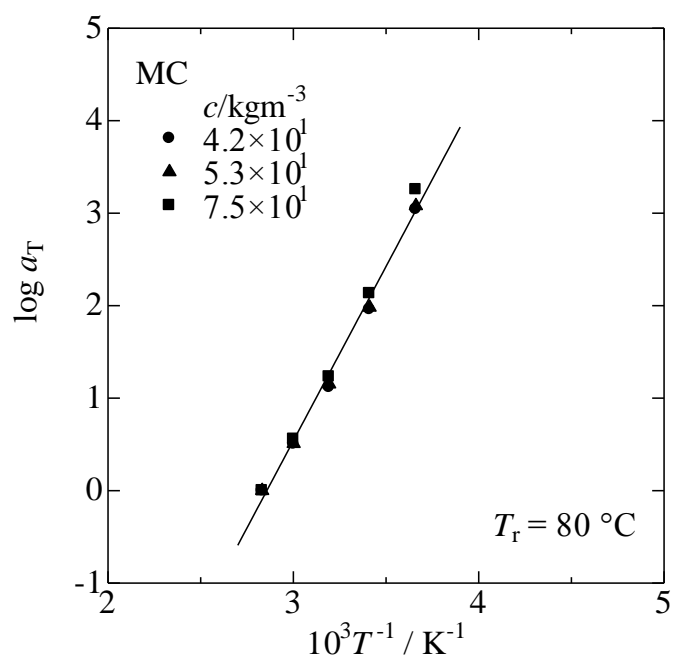


Figure 5

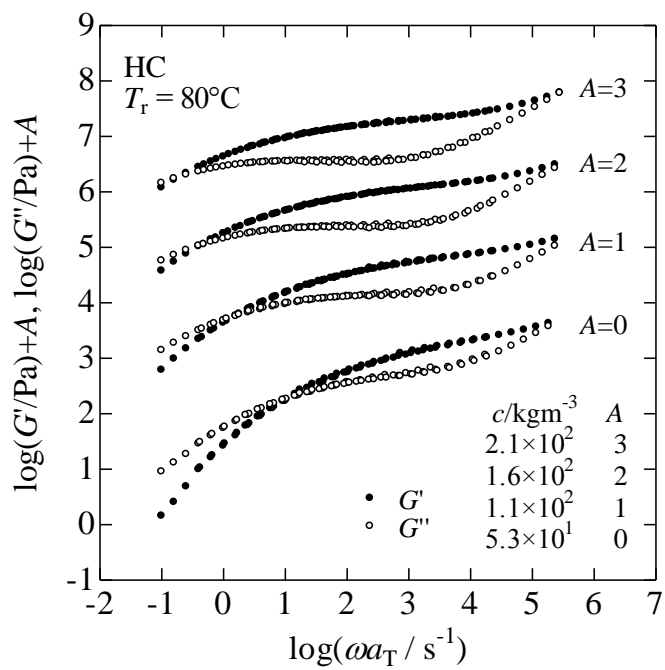


Figure 6

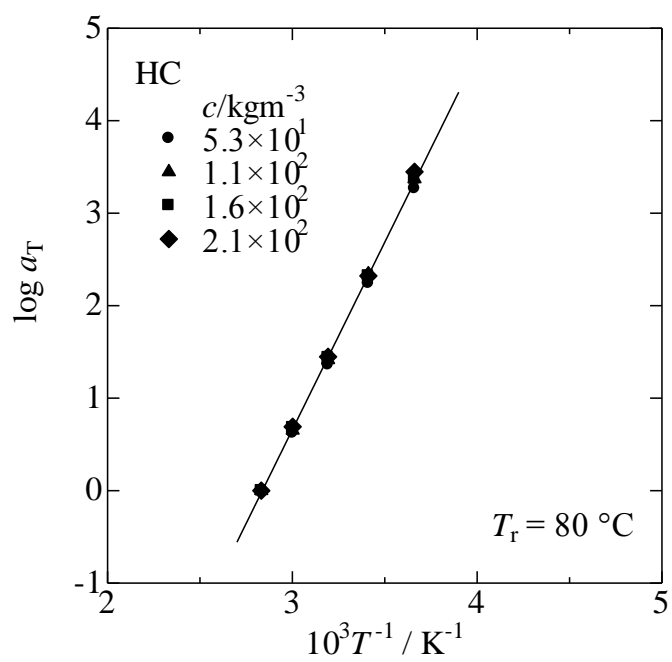


Figure 7

